Received: 16 September 2017 | Revised: 28 November 2017 | Accepted: 1 December 2017
DOI: 10.1002/rra.3245

RESEARCH ARTICLE

WILEY

Modelling upstream fish passage in standard box culverts: Interplay between turbulence, fish kinematics, and energetics

H. Wang | H. Chanson

School of Civil Engineering, The University of Queensland, Brisbane, QLD, Australia

Correspondence
H. Chanson, Professor in Civil Engineering, School of Civil Engineering, The University of Queensland, Brisbane, QLD 4072, Australia.
Email: h.chanson@uq.edu.au

Funding information
Australian Research Council, Grant/Award Number: LP140100225

Abstract

Box culverts are common hydraulic structures along rivers and streams, in rural and urban water systems. The expertise in fish-friendly culvert design is limited, sometimes leading to adverse impact on the catchment ecosystem or to uneconomical structures. Basic dimensional considerations highlight a number of key parameters relevant to any laboratory modelling of upstream fish passage, including the ratio of fish speed fluctuations to fluid velocity fluctuations, the ratios of fish dimensions to turbulent length scale, and the fish species. Alternately, the equation of conservation of momentum may be applied to an individual fish, yielding some deterministic estimate of instantaneous thrust and power expended during fish swimming, including the associated energy consumption. The rate of work required by the fish to deliver thrust is proportional to the cube of the local fluid velocity, and the model results demonstrate the key role of slow-velocity regions in which fish will minimize their energy consumption when swimming upstream.

KEYWORDS

bed slope effect, box culverts, dimensional analysis, energy considerations, fish-turbulence interplay, physical modelling, similitude, upstream fish passage

1 | INTRODUCTION

A culvert is a covered channel designed to allow the passage of flood waters beneath an embankment, for example, a roadway or railroad. Current designs are very similar to ancient designs, for example, Roman road culverts (Chanson, 2002; O'Connor, 1993) and characterized by some significant afflux at design flows (Henderson, 1966). The afflux is the rise in the upstream water level caused by the presence of the culvert, and it is a measure of upstream impoundment. In terms of hydraulic engineering, the optimum size is the smallest barrel size allowing for inlet control operation (Chanson, 1999; Herr & Bossy, 1965). The barrel, or throat, is the narrowest section of the culvert. The final culvert designs are very diverse, using various shapes and construction materials determined by stream width, peak flows, stream gradient, road direction, and minimum cost (Australian Standard, 2010; Hee, 1969; Henderson, 1966; Figure 1). In turn, this results in a wide diversity in flow patterns (Hee, 1969).

Although the culvert discharge capacity derives from hydrological and hydraulic engineering considerations, the final design often results in large velocities in the barrel, creating some fish passage barrier and loss in stream connectivity (Diebel, Fedora, Cogswell, & O'Hanley, 2015; Wyzga, Amirowicz, Radecki-Pawlik, & Zawiejska, 2009). During the last three decades, a recognition of the ecological impact of culverts on streams and rivers led to changes in culvert design guidelines (Behlke, Kane, McLeen, & Travis, 1991; Chorda, Larinier, & Font, 1995; Hajdukiewicz et al., 2017). For some applications, baffles may be installed along the barrel invert to provide some fish-friendly alternative (Chanson & Uys, 2016; Duguay & Lacey, 2014). Unfortunately, baffles can reduce drastically the culvert discharge capacity (Larinier, 2002; Olsen & Tullis, 2013).

The interactions between swimming fish and vortical structures were first mentioned by Leonardo Da Vinci (Keele, 1983, p. 185). These interactions are complicated, and naive "turbulence metrics cannot explain all the swimming path lines or behaviours" (Goettel, Atkinson, & Bennett, 2015). The turbulent flow patterns constitute a determining factor characterizing the capacity of the culvert structure to pass successfully targeted fish species. A seminal discussion emphasized the role of secondary flow motion (Papanicolaou & Talebbeydokhti, 2002).

Laboratory studies of fish swimming in turbulent flows are commonly be conducted. The hydraulic modelling aims to find optimal solutions of real-world problems (Novak & Cabelka, 1981). Major

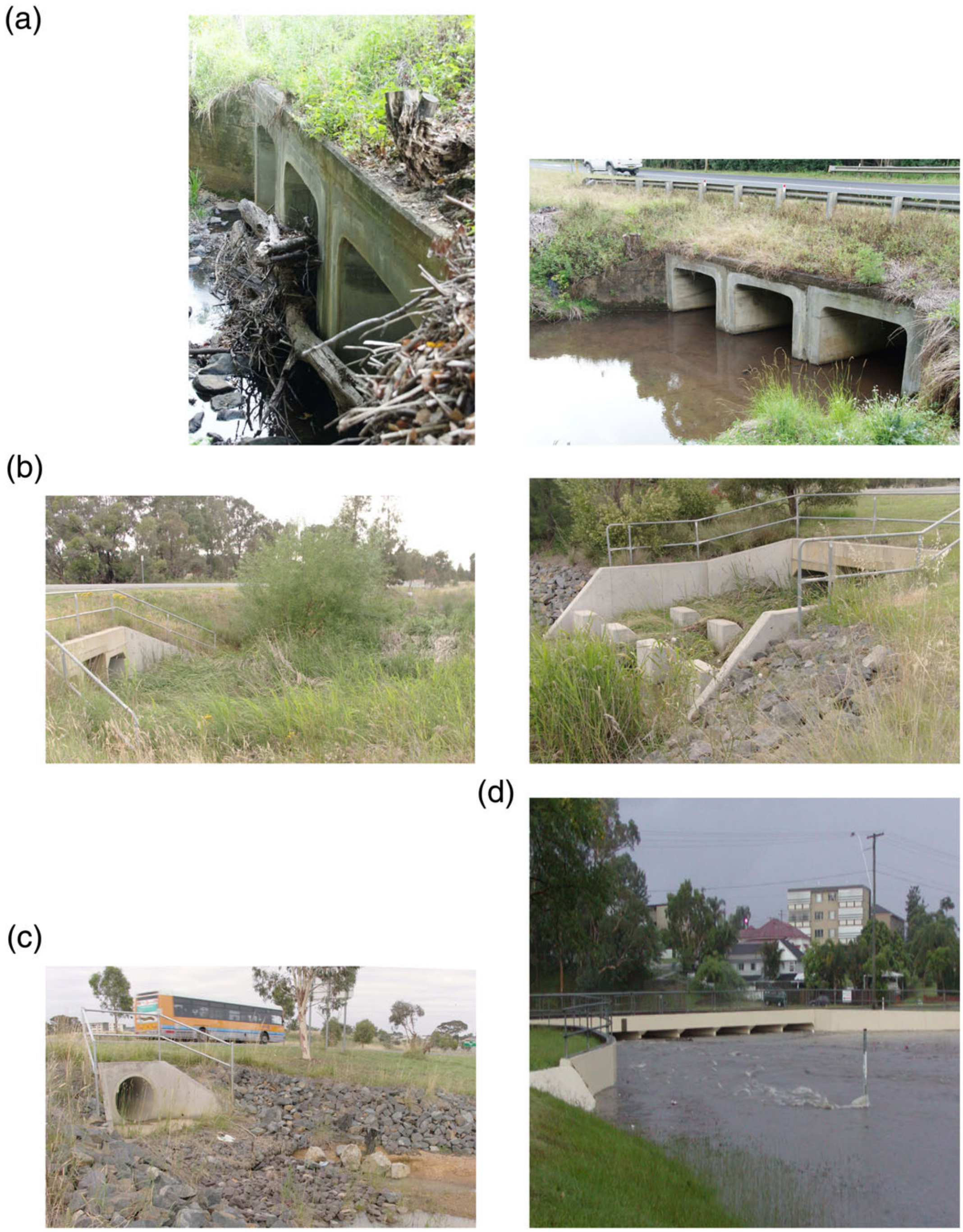

FIGURE 1 Standard culvert structures. (a) Inlet (left) and outlet (right) of a three cells box culverts in New South Wales (Australia). (b) Box culvert outlets in Australian Capital Territory. (c) Pipe culvert outlet in Australian Capital Territory. (d) Multicell box culvert operation in Brisbane (Australia) on December 31, 2001, early morning. Discharge estimated to 60–80 m^3/s ($Re \approx 2 \times 10^7$). Inlet with flood flow direction from right to left [Colour figure can be viewed at wileyonlinelibrary.com]

differences between up-scaled model estimates and prototype observations may result due to the lack of standardized methods (Cotel & Webb, 2015; Katopodis & Gervais, 2016). A recent contribution hinted that "a proper study of turbulence effects on fish behaviour should involve, in addition to turbulence energetics, consideration of fish dimensions in relation to the spectrum of turbulence scales" (Nikora, Aberle, Biggs, Jowett, & Sykes, 2003).

On another hand, fish tend to minimize their energy expenditure during upstream culvert passage and may use different strategies (Blake, 1983; Videler, 1993). Power and energy expenditure calculations were proposed (e.g., Behlke et al., 1991; Crower & Diplas, 2002), but current models lack detailed hydrodynamic and fish kinematic data for accurate results.

Herein, the modelling of upstream passage of fish in box culverts is reviewed, with a focus on the interplay between turbulence and fish, and the implications in terms of laboratory modelling and swimming energetics. Dimensional analysis provides a number of important dimensionless parameters relevant to laboratory studies, highlighting practical limitations for extrapolation. Fish kinematics and energetic considerations are developed in the context of fish passage in a culvert barrel. Energy consumption minimization is discussed during upstream fish passage, including the impact of barrel invert slope.

2 | LABORATORY STUDIES, SIMILARITY, AND DIMENSIONAL CONSIDERATIONS

In experimental fluid mechanics, a laboratory model study is to provide reliable predictions of the flow properties of the associated full-scale structure (Foss, Panton, & Yarin, 2007; Liggett, 1994; Novak & Cabelka, 1981). Any physical study in laboratory must be based upon the basic concept and principles of similitude, to ensure a reliable and accurate extrapolation of the laboratory model results. In any dimensional analysis of the hydrodynamics, the relevant dimensional parameters include the fluid properties, physical constants, channel geometry, and initial flow conditions (Henderson, 1966; Liggett, 1994). Considering the simplistic case of a steady turbulent flow in a box culvert barrel operating in free-surface flow, a dimensional analysis yields a series of relationships between the flow properties at a location (x, y, z) and the upstream flow conditions, channel geometry, and fluid properties:

$$d, \vec{V}, v', p, L_t, T_t, \ \ldots \ = \ F_1\left(x, y, z, B, k_s, \theta, h_b, L_b, d_1, V_1, {v_1}', \rho_w, \mu_w, \sigma, g, \ \ldots\right), \tag{1}$$

where d is the flow depth, V is the velocity, v' is a velocity fluctuation, p is the pressure, L_t and T_t are integral turbulent length and time scales, x, y, and z are respectively the longitudinal, transverse, and vertical coordinates, B is the channel width, k_s is the equivalent sand roughness height of the culvert barrel boundary, θ is the angle between the culvert invert and horizontal, h_b and L_b are respectively the height and longitudinal spacing of simplistic baffles, d_1, V_1, and ${v_1}'$ are respectively the inflow depth, velocity, and velocity fluctuation, ρ_w and μ_w are respectively the water density and dynamic viscosity, σ is the surface tension, and g is the gravity acceleration.

The Π-Buckingham theorem states that a dimensional equation with N dimensional variables may be simplified in an equation with N-3 dimensionless variables, when the mass, length, and time units are used among the N dimensional variables (Foss et al., 2007; Liggett, 1994). In turn, Equation 1 may be rewritten:

$$\frac{d}{d_c}, \frac{V_x}{V_c}, \frac{{v_x}'}{V_c}, \frac{p}{\rho_w \times g \times d_c}, \frac{L_t}{d_c}, T_t \times \sqrt{\frac{g}{d_c}} \ \ldots \ = F_2\begin{pmatrix} \frac{x}{d_c}, \frac{y}{d_c}, \frac{z}{d_c}, \\ \frac{B}{d_c}, \theta, \frac{k_s}{d_c}, \frac{h_b}{d_c}, \frac{L_b}{d_c}, \\ \frac{d_1}{d_c}, \frac{V_1}{\sqrt{g \times d_1}}, \frac{{v_1}'}{V_1}, \\ \rho_w \times \frac{V \times D_H}{\mu_w}, \frac{g \times {\mu_w}^4}{\rho_w \times \sigma^3}, \ \ldots \end{pmatrix}, \tag{2}$$

where d_c is the critical flow depth: $d_c = (Q^2/(g \times B^2)^{1/3})$, V_c is the critical flow velocity, Q is the water discharge, and D_H is the equivalent pipe diameter, or hydraulic diameter. In Equation 2, right-hand side term, the 7th term is the inflow Froude number Fr_1, and the 8th and 9th terms are the Reynolds number Re and Morton number Mo, respectively. Herein, the Morton number is introduced because it is a constant in most hydraulic model studies, when air and water are used in both laboratory experiment and prototype flows.

Traditionally, hydraulic model studies are performed using geometrically similar model (Chanson, 1999; Liggett, 1994). If any geometric, kinematic, or dynamic similarity is not fulfilled, scale effects may take place. Scale effects yield discrepancies between the model data extrapolation and prototype performances. In a physical model, true similarity can be achieved only if each dimensionless parameter or Π-term has the same value in both model and prototype:

$$\begin{aligned} Fr_m &= Fr_p \\ Re_m &= Re_p \\ Mo_m &= Mo_p, \end{aligned} \tag{3}$$

where the subscripts m and p refer to the laboratory model and full-scale conditions, respectively. Open channel flows including culvert flows are traditionally investigated based upon a Froude similarity because gravity effects are important (Henderson, 1966; Liggett, 1994; Novak & Cabelka, 1981). In practice, the Froude and Morton similarities are simultaneously employed with the same fluids, air and water, used at full scale and in laboratory. In turn, the Reynolds number is grossly underestimated in laboratory: for example, the Reynolds numbers of about 2×10^5 and 5×10^3 in the laboratory models seen in Figure 2a,b, respectively, compared to a full-scale flow seen in Figure 1 d corresponding to $Re \approx 2 \times 10^7$.

A dimensional analysis may be similarly conducted for the fish motion in a turbulent flow (Alexander, 1982; Blake, 1983). Considering the simplified motion of a fish travelling upstream in a prismatic box culvert barrel with a steady turbulent flow, dimensional considerations yield a series of relationships between the fish motion characteristics at a location (x, y, z), fish characteristics, channel boundary conditions, turbulent flow properties, fluid properties, and physical constants:

$$\vec{U}, u', O_2, \tau_f, \ \ldots \ = \ F_3\begin{pmatrix} x, y, z, \\ L_f, l_f, h_f, \rho_f, \text{specie}, \\ B, k_s, \theta, h_b, L_b, \\ d, V, v', L_t, T_t, \\ \rho_w, \mu_w, \sigma, g, \ldots \end{pmatrix}, \tag{4}$$

where U is the fish speed for a fixed observer positive upstream because this study is concerned with the upstream fish passage, u' is a fish speed fluctuation, O_2 is the oxygen consumption, τ_f is the fish response time, L_f, l_f, and h_f are respectively the fish length, thickness, and height, and ρ_f is the fish density. Note that Equation 4 ignores the effects of fish fatigue. The application of the Π-Buckingham theorem implies that Equation 4 may be rewritten in dimensionless form as:

$$\frac{U}{V_c}, \frac{u'}{v'}, O_2, \frac{\tau_f}{T_t}, \ \ldots \ = \ F_4\begin{pmatrix} \frac{x}{d_c}, \frac{y}{d_c}, \frac{z}{d_c}, \\ \frac{L_f}{L_t}, \frac{l_f}{L_t}, \frac{h_f}{L_t}, \frac{\rho_f}{\rho_w}, \text{specie}, \\ \frac{B}{d_c}, \frac{k_s}{d_c}, \theta, \frac{h_b}{d_c}, \frac{L_b}{d_c}, \\ Fr, \ Re, Mo, \frac{L_t}{d_c}, T_t \times \sqrt{\frac{g}{d_c}}, \ldots \end{pmatrix}. \tag{5}$$

The result, that is, Equation 5, highlights a number of key parameters and variables relevant to the upstream fish passage in a turbulent

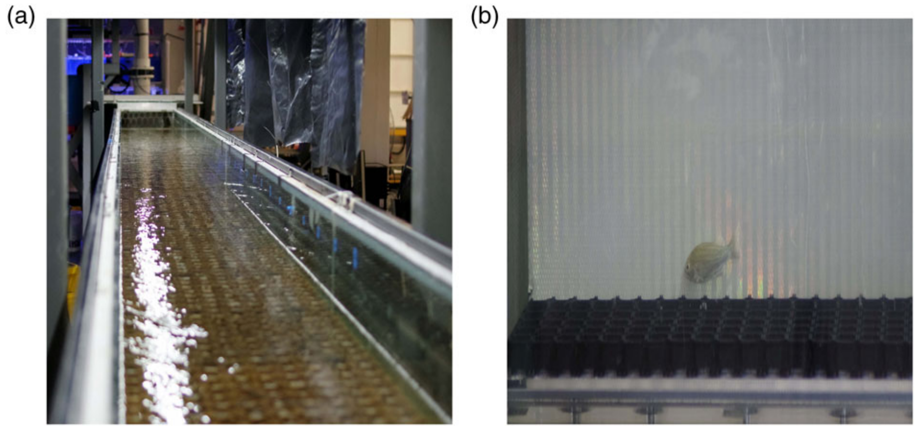

FIGURE 2 Laboratory studies of fish passage in culvert barrel with roughened invert. (a) Open channel flow in a 12-m-long channel: B = 0.5 m, θ = 0, Q = 0.026 m^3/s, d = 0.12 m, and Re = 2 × 10^5, flow direction from background to foreground. (b) Recirculation water tunnel: B = 0.25 m, θ = 0, V ~ 0.05 m/s, d = 0.26 m, flow motion from left to right [Colour figure can be viewed at wileyonlinelibrary.com]

culvert barrel flow. These include the ratio u'/v' of fish speed fluctuations to fluid velocity fluctuations, the ratio τ_f/T_t of fish response time to turbulent time scales, the ratios of fish dimension to turbulent length scale, and the fish species. From the point of view of fish motion in turbulent culvert flow, the laboratory model will behave like the full-scale culvert if the key relevant dimensionless parameters are identical in laboratory and at full scale.

A few studies recorded quantitative detailed characteristics of both fish motion and fluid flow (Nikora et al., 2003; Plew, Nikora, Larne, Sykes, & Cooper, 2007). Fewer investigations reported fish speed fluctuations and fluid velocity fluctuations, and fish response time and integral time scales (Wang, Chanson, Kern, & Franklin, 2016). Yet these results suggested that a number of key parameters, including the ratios u'/v', τ_f/T_t, and L_f/L_t, are scale dependant when the same fish are used in laboratory and in the field. In other words, a complete similarity between laboratory data and full-scale observations may be unattainable, and one must seek either an incomplete similitude, approximate estimate, or alternative approach.

3 | FISH KINEMATICS AND ENERGY CONSUMPTION

A different modelling technique may be derived by analogy with sport physics (Clanet, 2013). Considering a fish swimming upstream in a culvert barrel, detailed records of its motion and trajectory provide critical information on fish locomotion dynamics that can be used to calculate energy expenditure, with significant implications for the understanding of energetics and biomechanics of aquatic propulsion (Lauder, 2015). Assuming some carangiform propulsion, the primary forces acting on each fish include the thrust force, gravity force, buoyancy force, shear/drag force, lift force, and virtual mass force. Newton's law of motion applied to a fish yields:

$$m_f \times \frac{d\overrightarrow{U}}{dt} = \overrightarrow{F}_{thrust} - \overrightarrow{F}_{drag} - \overrightarrow{F}_{inertial} - m_f \times \overrightarrow{g} + \overrightarrow{F}_{lift} + \overrightarrow{F}_{buoyancy}, \quad (6)$$

where m_f is the fish mass. The buoyancy and lift forces act along the normal direction: that is, perpendicular to the flow streamlines, and their contribution in the longitudinal x-direction is zero. The drag force acts along the flow direction. It includes a skin friction component plus a form drag component. The skin friction is associated with a boundary layer development along the fish surfaces, whereas the form drag is linked to the vortex development and turbulence dissipation in the wake of the fish (Schultz & Webb, 2002). For a fish swimming upstream, in a stream tube and neglecting the virtual mass force, Newton's law of motion applied to the fish in the longitudinal x-direction yields in first approximation:

$$m_f \times \frac{\partial U_x}{\partial t} = F_{thrust} - F_{drag} - m_f \times g \times \sin\theta, \quad (7)$$

where the main forces acting on the fish are the thrust F_{thrust} and drag force F_{drag} and the last term is the gravity force component in the flow direction. For a fish in motion, the drag force may be expressed as:

$$F_{drag} = C_d \times \rho_w \times \left(\overline{U_x + V_x}\right)^2 \times A_f, \quad (8)$$

where C_d is the drag coefficient, U_x is the longitudinal fish speed component positive upstream, V_x is the longitudinal fluid velocity component at the fish location positive downstream, and A_f is the projected area of the fish. $\overline{U_x + V_x}$ is the mean relative fish speed over a control volume, basically a stream tube, selected such that the lateral surfaces are parallel to the streamlines and that it extends up to the wake region's downstream end (Alexander, 1982; Lighthill, 1969; Figure 3b).

An estimate of drag coefficient C_d might be derived from high-resolution trajectory data when the fish drifts. During drifting in a horizontal channel, the fish deceleration is driven by the drag force, and Newton's law of motion becomes (Blake, 1983):

$$m_f \times \frac{\partial U}{\partial t} \approx -C_d \times \rho_w \times \left(\overline{U_x + V_x}\right)^2 \times A_f. \quad (9)$$

In turn, the product $C_d \times A_f$ may be derived from the rate of deceleration and relative fish speed, assuming implicitly that the form drag is identical during glide and during thrust and unaffected by body motion. Figure 3a shows an example of time-variation of fish speed and acceleration during a drift event, for a fish swimming next to the corner

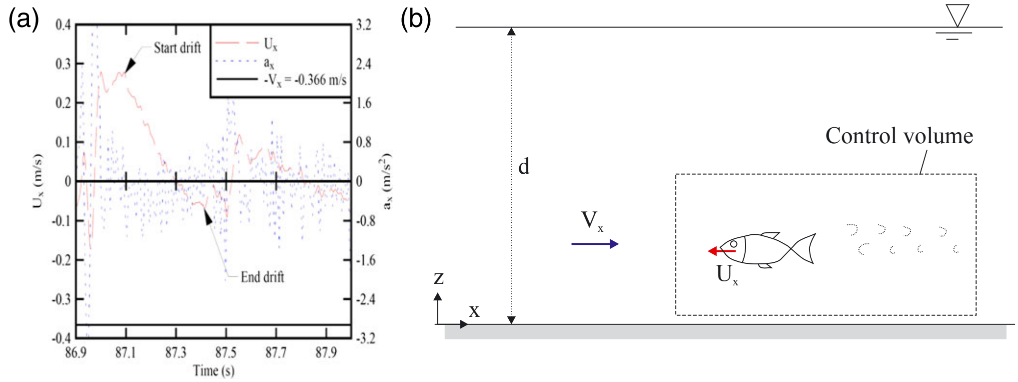

FIGURE 3 Estimate of drag coefficient during fish drift. (a) Time-variation of Duboulay's rainbowfish speed and acceleration during a drift event—Data: Wang, Chanson, et al. (2016), individual no. 22, m_f = 3.6 g, L_f = 72 mm, fish swimming along a rough sidewall, local flow conditions: V_x = +0.366 m/s, v_x' = 0.315 m/s, θ = 0. (b) Definition sketch of drag force estimate on a fish swimming upstream against the current [Colour figure can be viewed at wileyonlinelibrary.com]

between a rough sidewall and rough invert. For that particular drift event, $C_d \times A_f = 4.3 \times 10^{-3}$ m^2.

The rate of working of the fish and its time-variations may be estimated with a fine temporal scale, within the time-series accuracy (Equation 7). The power that the fish expends during swimming is the product of the thrust and relative fish speed. Neglecting efforts spent during lateral and upward motion, the mean rate of work by the fish is (Behlke et al., 1991; Lighthill, 1960):

$$P = F_{thrust} \times (U_x + V_x), \tag{10}$$

with P the instantaneous power spent by the fish to provide thrust and ($U_x + V_x$) is the local relative fish speed, at the fish location. Combining with Equations 7 and 8, it yields:

$$P = \left(m_f \times \frac{\partial U}{\partial t} + C_d \times \rho_w \times \left(\overline{U_x + V_x}\right)^2 \times A_f + m_f \times g \times \sin\theta \right) \times (U_f + V_x). \tag{11}$$

Equation 11 expresses the instantaneous rate of working by the fish, to counterbalance the effects of inertia, drag, and gravity. It may be calculated from measured fish acceleration, fish speed, and fluid velocity time series. The finding shows in particular that the rate of working increases with increasing relative fish speed, and the drag component increases with the cube of the relative fish speed $(U_x + V_x)^3$.

The energy spent by the moving fish during a time T is

$$E = \int_{t=0}^{T} P \times dt, \tag{12a}$$

where t is the time. Combining with Equation 11:

$$E = \int_{t=0}^{T} \left(m_f \times \frac{\partial U}{\partial t} + C_d \times \rho_w \times \left(\overline{U_x + V_x}\right)^2 \times A_f + m_f \times g \times \sin\theta \right) \times (U_f + V_x) \times dt. \tag{12b}$$

If T is the transit time of a fish in a culvert structure, Equation 12 gives a quantitative estimation of the work spent by the fish to navigate upstream through the culvert, although it does not account for any heat transfer and fish metabolism. Note however that any application of Equation 12 relies upon detailed time series data of fish acceleration, fish speed, and fluid velocity.

Application

Detailed fish kinematic data and fluid dynamics data were obtained in a 12-m-long and a 0.5-m-wide open channel equipped with a rough invert, rough left sidewall, and smooth right sidewall (Wang, Chanson, et al., 2016). The rough boundaries consisted of rubber mats with square patterns: 0.0482 × 0.0482 m for the bed and 0.0375 × 0.0375 m for the left sidewall, the water surface elevation being measured from the top of the rubber mats. The dimensionless boundary shear stress, expressed in terms of equivalent Darcy–Weisbach friction factor, was about f = 0.07 to 0.12, compared to f = 0.015 to 0.017 for the smooth polyvinyl chloride (PVC) bed configuration in the same flume. Fish swimming tests were performed with juvenile silver perch (*Bidyanus bidyanus*) and adult Duboulay's rainbowfish (*Melanotaenia duboulayi*) in the rough bed and rough sidewall channel at 24.5 ± 0.5 °C (Wang, Chanson, et al., 2016). Figure 4a presents a typical individual fish trajectory time series, with the fish mass and length, and flow conditions listed in caption, and with *x* the longitudinal co-ordinate positive downstream and *x* the vertical elevation above the bed. For that time series, the fish swam against the current, next to the rough corner of the channel, exhibiting a carangiform locomotion. Visual observations and velocity time series showed that the fish motion consisted of some quasi-stationary motion where fish speed fluctuations were small and short upstream bursts facilitated by a few strong tail-beats. The instantaneous power and energy spent by the moving fish to provide thrust were calculated for the trajectory data seen in Figure 4a. The results are shown in Figure 4b. On average, the mean rate of work by the fish was 0.21 W, with a standard deviation of 0.065 W. The first, second, and third quartiles were 0.175, 0.207, and 0.241 W, respectively. The maximum instantaneous power spent by the fish to provide thrust reached 3.3 W. Overall the power distribution was skewed with a preponderance of small values relative to the mean (Figure 4c). The energy spent by the fish to provide thrust was 21 J for the entire trajectory (100-s long).

The experimental data may be extrapolated to a 10-m-long box culvert barrel, which would be typical of small road culvert structures

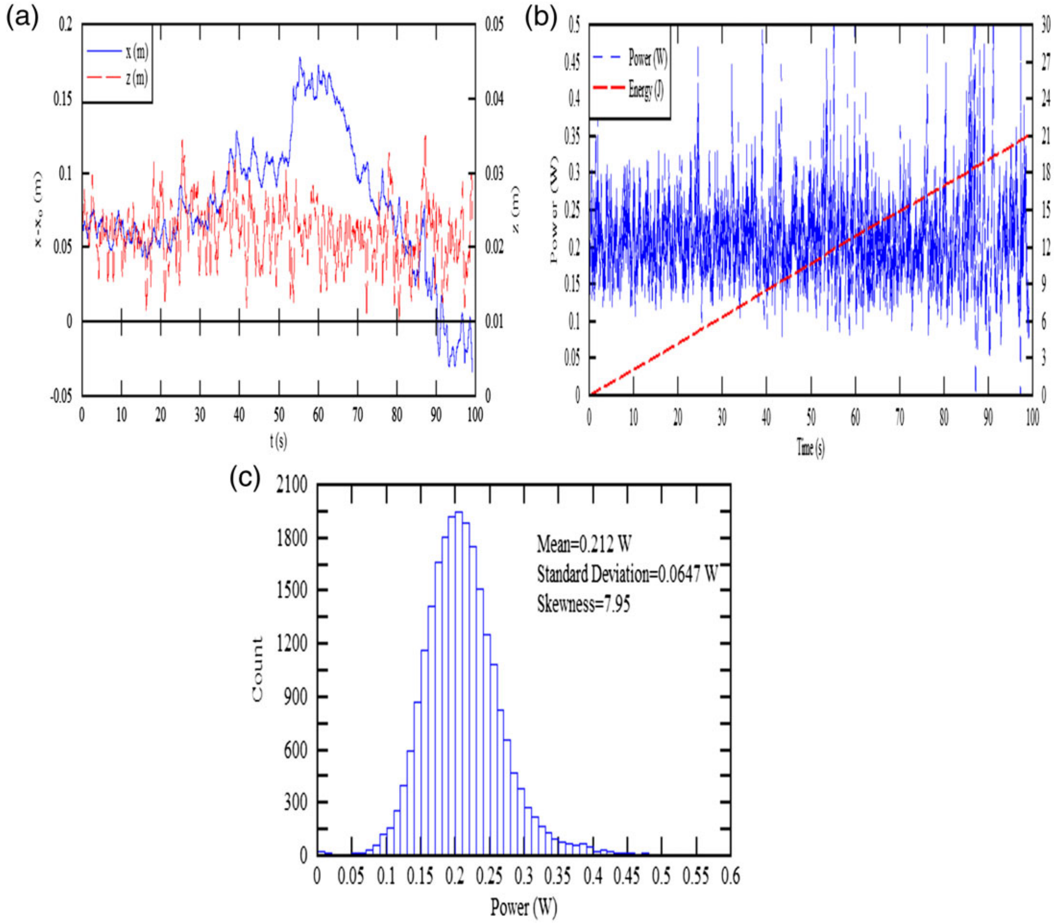

FIGURE 4 Time-variations of fish position and power expended during fish swimming in a 12-m-long and a 0.5-m-wide open channel—Data: Wang, Chanson, et al. (2016), Duboulay's rainbowfish no. 22, m_f = 3.6 g, L_f = 72 mm, $C_d \times A_f = 4.3 \times 10^{-4}$ m^2—Q = 0.0261 m^3/s, θ = 0, fish swimming along a rough sidewall, local fluid flow conditions: d = 0.14 m, V_x = +0.366 m/s, v_x' = 0.315 m/s. (a) Time-variations of longitudinal and vertical fish position. (b) Time-variations of instantaneous power P and energy E spent by the fish to provide longitudinal thrust during the above trajectory. (c) Probability distribution function of instantaneous power P spent by the fish to provide longitudinal thrust during the above trajectory [Colour figure can be viewed at wileyonlinelibrary.com]

in eastern Australia, equipped similarly with rough barrel boundary. Assuming a similar behaviour to the trajectory data shown in Figure 4 a, the energy spent by the fish to provide thrust would be 2,130 J (i. e., 509 calories) to negotiate the 10-m-long horizontal culvert barrel.

4 | DISCUSSION

Although basic dimensional analysis points to the intrinsic limitations of laboratory investigations at small scales, energetic considerations paved the way for a deterministic method to quantify accurately the power and energy expended by a moving fish, to counterbalance the drag, inertia, and gravity forces, as the fish swims upstream in a culvert barrel. The analytical model provides an improved understanding of the implications of propulsion type and associated power requirements. The mathematical development shows in particular that the work spent by the moving fish is proportional to the cube of the relative fish speed (Equation 12). Thus, it is strongly linked to the local fluid velocity V_x. The results may be applied to develop new physically based design guidelines and to account for the effects of bed slope.

Design considerations

Basic reasoning showed that the rate of work and work required to deliver thrust is proportional to the cube of the local fluid velocity (Equations 11 and 12). Thus, fish will minimize their energy consumption by swimming upstream in slow-velocity regions. A reduction in 20% in fluid velocity is associated with a 60% reduction in power that the fish expends during swimming. The result is valid in both horizontal and sloping barrel invert, implying that fish-friendly culvert design must provide sizeable slow-velocity regions to facilitate upstream fish passage.

Fish-friendly culvert designs may consist of channel configurations that provide sizeable slow-velocity regions and maximize secondary currents all along the culvert barrel, without increasing the total head loss in the structure. Wang, Beckingham, Johnson, Kiri, and Chanson (2016) tested a design consisting of a very rough bed and a very rough sidewall, for the full length of the barrel. Detailed velocity measurements showed the existence of sizeable slow-velocity regions next to the left rough sidewall and at the corner between the rough bed and sidewall, which might be suitable to the upstream passage of small body mass fish. Wang, Uys, and Chanson (2017) tested several baffles

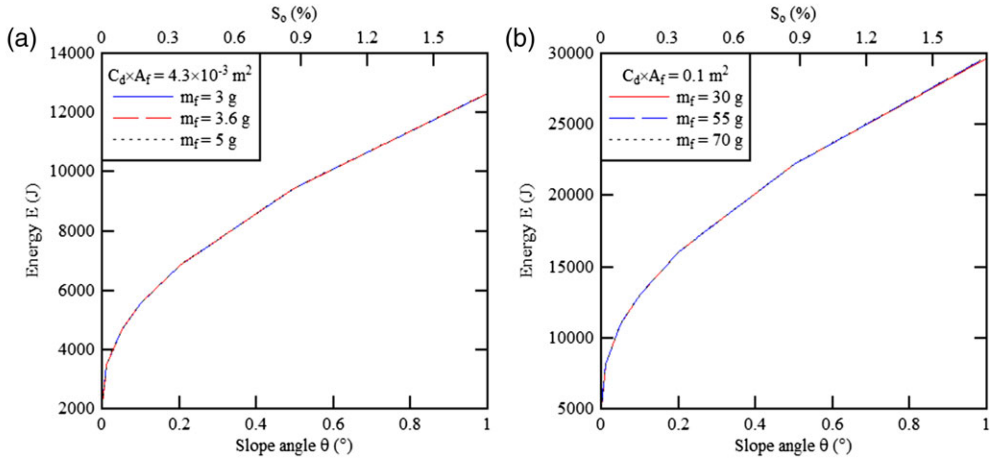

FIGURE 5 Energy E spent by a fish to provide longitudinal thrust along a 10-m-long culvert barrel as a function of the bed slope, assuming a fish trajectory shown in Figure 4a. (a) Small fish no. 1: m_f = 3–5 g, $C_d \times A_f = 4.3 \times 10^{-3}$ m^2. (b) Small fish no. 2: m_f = 30–70 g, $C_d \times A_f$ = 0.1 m^2 [Colour figure can be viewed at wileyonlinelibrary.com]

designs in a standard box culvert model. One configuration, a series of corner baffles, assisted with the development of recirculation zones between each baffle, with a small increase (10%) in afflux at design discharge, and might be suitable to small-body-mass fish species.

Effect of bed slope on culvert design

Kinematic and energetic considerations show that the culvert bed slope impacts on the energy spent by the fish during upstream culvert passage. Additional energy is required with increasing slope θ because of the increased contribution of the gravity force to the dissipated power by the fish to provide thrust, as well as by the increase in fluid velocity, hence in relative fish speed. This might be particularly detrimental to weak-swimming fish species.

The effect of bed slope on the rate of working by the fish is two-fold. First, it increases the gravity force component ($m \times g \times \sin\theta$). Second, a positive downward bed slope will yield an increased fluid velocity. In first approximation, the fluid velocity increases as (see Appendix A):

$$\frac{\partial V}{\partial \theta} \approx \frac{1}{3} \times \sqrt[3]{\frac{8 \times g}{f} \times q \times (\sin\theta)^{-2/3}}, \tag{13}$$

where f is the Darcy–Weisbach friction factor, q is the discharge per unit width area, and g is the gravity acceleration.

Assuming that the fish trajectory is unaffected by the channel slope and that the local flow conditions satisfy Equation 13, the effects of bed slope θ on the rate of working and the energy spent by the fish to provide thrust may be tested (Equations 11 and 12). The calculations may be extended to a broader range of bed slope for a 10-m-long culvert, assuming that the fish trajectory would follow the trajectory shown in Figure 4a, irrespective of fish mass and bed slope. Herein, calculations were conducted for bed slope θ = 0 to 1°: that is, for $S_o = \sin\theta$ = 0 to 1.75%. Such a range of slopes would encompass most typical mild slope flood plains, whereas the steepest slopes would correspond to a steep flood plain. Results are shown in Figure 5, for two types of small fish, defined by the fish mass m_f and product $C_d \times A_f$ of drag coefficient by projected area. The first type would be typical of very small fish species, such as Duboulay's rainbowfish (*M. duboulayi*), whereas the second type would correspond to slightly larger fish species. Within the implicit assumptions, the results suggest that the channel slope affects significantly the instantaneous power and energy spent by the fish to provide thrust during upstream culvert passage (Figure 5). The required energy increases monotonically with the bed slope. For this culvert system, the work spent by the fish is about 6 times larger when the bed slope increases from S_o = 0 to 1.75% for both fish types 1 and 2.

5 | CONCLUSION

Culvert structures may constitute barriers, adversely affecting the upstream passage of many fish species, with direct implications in terms of catchment biodiversity. It is argued that fish-turbulence interactions may facilitate upstream fish migration, although any optimum design must be based upon a detailed characterization of both hydrodynamics and fish kinematics. Dimensional considerations highlighted a number of key relevant parameters to assist with upstream fish passage and its laboratory modelling. These included the ratio of fish speed fluctuations to fluid velocity fluctuations, the ratio of fish response time to turbulent time scales, the ratios of fish dimension to turbulent length scale, and the fish species. The latter is a most important variable, because design guidelines developed for one species might be inadequate for other species. Basically, any physical experiment must be designed in such a manner that these key dimensionless parameters are the same in laboratory and full-scale culvert structure.

The application of the equation of conservation of momentum provides a deterministic method to quantify the fish thrust and instantaneous power expended by a fish to provide thrust. The power and work required to deliver thrust is proportional to the cube of the local fluid velocity. In a culvert barrel, fish can minimize their energy consumption by swimming upstream in slow-velocity regions. Using kinematic data recorded with fine spatial and temporal resolution, the associated energy consumption may be estimated, and the effects of bed slope can be tested. It is believed that the present approach paves the way for an improved knowledge of fish-turbulence interplay relevant to upstream fish passage in culverts. This is significant given the recent efforts to design cost-effective fish-friendly box culverts.

In principle, the proposed approach is general and may be applied to other conditions, such small hydropower systems, baffled chutes, and small groyne systems. In practice, however, reliable results require relatively simple geometries, for which the relative fish speed, that is, both the fluid velocity and fish speed, can be accurately determined and measured.

ACKNOWLEDGEMENTS

The authors thank their students Ramith Fernando, Rui Shi, Amelia Tatham, Joseph Dowling, Urvisha Kiri, Caitlyn Johnson, and Laura Beckingham (UQ). They further acknowledge Dr. Pippa Kern, Dr. Matthew Gordos, and Professor Craig Franklin for helpful discussions and inputs. The financial support through the Australian Research Council (Grant LP140100225) is acknowledged.

DECLARATIONS OF INTEREST

The authors have no financial interest or benefit that has arisen from the direct applications of the research.

ORCID

H. Wang http://orcid.org/0000-0002-3542-8416
H. Chanson http://orcid.org/0000-0002-2016-9650

REFERENCES

Alexander, R. M. (1982). *Locomotion of animals*. USA: Chapman and Hall.

Australian Standard (2010). Precast reinforced concrete box culverts. In *Part 1: Small culverts (not exceeding 1200 mm span and 1200 mm height)* (2nd ed.) *Standards Australia AS 1597.1-2010* (pp. 245). Canberra ACT, Australia: Standards Australia Publications.

Behlke, C. E., Kane, D. L., McLeen, R. F., & Travis, M. T. (1991). Fundamentals of culvert design for passage of weak-swimming fish. Report FHW A-AK-RD-90-10, Department of Transportation and Public Facilities, State of Alaska, Fairbanks, USA, 178 pp.

Blake, R. W. (1983). *Fish locomotion*. UK: Cambridge University Press.

Chanson, H. (1999). *The Hydraulics of Open Channel Flow: An Introduction*. London, UK: Edward Arnold. [ISBN 0 340 74067 1].

Chanson, H. (2002). Hydraulics of a large culvert beneath the Roman aqueduct of Nîmes. *Journal of Irrigation and Drainage Engineering, ASCE*, *128*(5), 326–330. https://doi.org/10.1061/(ASCE)0733-9437(2002)128.

Chanson, H., & Uys, W. (2016). Baffle designs to facilitate fish passage in box culverts: A preliminary study. Proceedings of 6th IAHR International Symposium on Hydraulic Structures, Hydraulic Structures and Water System Management, Portland OR, USA, 295-304 (DOI: 10.15142/T300628160828).

Chorda, J., Larinier, M., & Font, S. (1995). Le Franchissement par les Poissons Migrateurs des Buses et Autres Ouvrages de Rétablissement des Ecoulements Naturels lors des Aménagements Routiers et Autoroutes. Etude Expérimentale. Rapport HYDRE n°159—GHAAPPE n°95-03, Groupe d'Hydraulique Appliquée aux Aménagements Piscicoles et à la Protection de l'Environnement, Service d'Etudes Techniques des Routes et Autoroutes, Toulouse, France, 116 pp (in French).

Clanet, C. (2013). Sports Physics. *Editions de l'Ecole Polytechnique*. Palaiseau, France, 633 pp.

Cotel, A. J., & Webb, P. W. (2015). Living in a turbulent world—A new conceptual framework for the interactions of fish and eddies. *Integrative and Comparative Biology*, *55*(4), 662–672.

Crower, D. W., & Diplas, P. (2002). Vorticity and circulation: Spatial metrics for evaluating flow complexity in stream habitats. *Canadian Journal of Fisheries and Aquatic Sciences*, *59*, 633–645.

Diebel, M. W., Fedora, M., Cogswell, S., & O'Hanley, J. R. (2015). Effects of road crossings on habitat connectivity for stream-resident fish. *River Research and Applications*, *31*, 1251–1261.

Duguay, J., & Lacey, R. W. J. (2014). Effect of fish baffles on the hydraulic roughness of slip-lined culverts. *Journal of Hydraulic Engineering, ASCE*, *141*(1), Paper 04014065,), 10. https://doi.org/10.1061/(ASCE)HY.1943-7900.0000942.

Foss, J. F., Panton, R., & Yarin, A. (2007). Nondimensional representation of the boundary-value problem. In C. Tropea, A. L. Yarin, & J. F. Foss (Eds.), Part A, Chapter 2, *Springer handbook of experimental fluid mechanics* (pp. 33–82). Heidelberg, Germany: Springer.

Goettel, M. T., Atkinson, J. F., & Bennett, S. J. (2015). Behavior of western blacknose dace in a turbulence modified flow field. *Ecological Engineering*, *74*, 230–240.

Hajdukiewicz, H., Wyżga, B., Zawiejska, J., Amirowicz, A., Oglęcki, P., & Radecki-Pawliki, A. (2017). Assessment of river hydromorphological quality for restoration purposes: An example of the application of RHQ method to a Polish Carpathian river. *Acta Geophysica*, *65*, 423–440. https://doi.org/10.1007/s11600-017-0044-7.

Hee, M. (1969). Hydraulics of culvert design including constant energy concept. Proc. 20th Conf. of Local Authority Engineers, Dept. of Local Government, Queensland, Australia, paper 9, 1-27.

Henderson, F. M. (1966). *Open channel flow*. New York, USA: MacMillan Company.

Herr, L. A., & Bossy, H. G. (1965). Hydraulic Charts for the Selection of Highway Culverts. *Hydraulic Eng. Circular*, US Dept. of Transportation, Federal Highway Admin., HEC No. 5, December.

Katopodis, C., & Gervais, R. (2016). Fish swimming performance database and analyses. DFO CSAS Research Document No. 2016/002, Canadian Science Advisory Secretariat, Fisheries and Oceans Canada, Ottawa, Canada, 550 pp.

Keele, K. D. (1983). *Leonardo Da Vinci's elements of the science of man*. USA: Academic Press.

Larinier, M. (2002). Fish passage through culverts, rock weirs and estuarine obstructions. *Bulletin Français de Pêche et Pisciculture*, *364*(18), 119–134.

Lauder, G. V. (2015). Fish locomotion: Recent advances and new directions. *Annual Review of Marine Science*, *7*, 521–545. https://doi.org/10.1146/annurev-marine-010814-015614.

Liggett, J. A. (1994). *Fluid mechanics*. New York, USA: McGraw-Hill.

Lighthill, M. J. (1960). Note on the swimming of slender fish. *Journal of Fluid Mechanics*, *9*, 305–317.

Lighthill, M. J. (1969). Hydromechanics of aquatic animal propulsion. *Annual Review of Fluid Mechanics*, *1*, 413–446.

Nikora, V. I., Aberle, J., Biggs, B. J. F., Jowett, I. G., & Sykes, J. R. E. (2003). Effects of fish size, time-to-fatigue and turbulence on swimming performance: A case study of Galaxias maculatus. *Journal of Fish Biology*, *63*, 1365–1382.

Novak, P., & Cabelka, J. (1981). *Models in hydraulic engineering. Physical principles and design applications* (pp. 459). London, UK: Pitman Publ.

O'Connor, C. (1993). *Roman bridges* (pp. 235). Cambridge, UK: Cambridge University Press.

Olsen, A., & Tullis, B. (2013). Laboratory study of fish passage and discharge capacity in slip-lined, baffled culverts. *Journal of Hydraulic Engineering, ASCE*, *139*(4), 424–432.

Papanicolaou, A. N., & Talebbeydokhti, N. (2002). Discussion of turbulent open-channel flow in circular corrugated culverts. *Journal of Hydraulic Engineering, ASCE*, *128*(5), 548–549.

Plew, D. R., Nikora, V. I., Larne, S. T., Sykes, J. R. E., & Cooper, G. G. (2007). Fish swimming speed variability at constant flow: Galaxias maculatus. *New Zealand Journal of Marine and Freshwater Research*, *41*, 185–195. https://doi.org/10.1080/00288330709509907.

Schultz, W. W., & Webb, P. W. (2002). Power requirements of swimming: Do new methods resolve old questions? *Integrative and Comparative Biology*, *42*, 1018–1025.

Videler, J. J. (1993). *Fish swimming*. London, UK: Chapman & Hall.

Wang, H., Beckingham, L. K., Johnson, C. Z., Kiri, U. R., & Chanson, H. (2016). Interactions between large boundary roughness and high inflow turbulence in open channel: A physical study into turbulence properties to enhance upstream fish migration. Hydraulic Model Report No. CH103/16, School of Civil Engineering, The University of Queensland, Brisbane, Australia, 74 pp.

Wang, H., Chanson, H., Kern, P., & Franklin, C. (2016). Culvert hydrodynamics to enhance upstream fish passage: Fish response to turbulence. In G. Ivey, T. Zhou, N. Jones, & S. Draper (Eds.), *Proceedings of 20th Australasian Fluid Mechanics Conference, Australasian Fluid Mechanics Society*. Perth WA, Australia: Australasian Fluid Mechanics Society. 5-8 December, Paper 682, 4 pp.

Wang, H., Uys, W., & Chanson, H. (2017). Alternative mitigation measures for fish passage in standard box culverts: Physical modelling. *Journal of Hydro-environment Research, IAHR*,Vol *16* (DOI: https://doi.org/10.1016/j.jher.2017.03.001) (In Press).

Wyzga, B., Amirowicz, A., Radecki-Pawlik, A., & Zawiejska, J. (2009). Hydromorphological conditions, potential fish habitats and the fish community in a mountain river subjected to variable human impacts, the Czarny Dunajec, Polish Carpathians. *River Research and Applications*, *25*(5), 517–536. https://doi.org/10.1002/rra.1237.

How to cite this article: Wang H, Chanson H. Modelling upstream fish passage in standard box culverts: Interplay between turbulence, fish kinematics, and energetics. *River Res Applic*. 2018;34:244–252. https://doi.org/10.1002/rra.3245

APPENDIX A

RELATIONSHIP BETWEEN FLUID VELOCITY AND BED SLOPE IN A BOX CULVERT

At uniform equilibrium in an open channel, the water depth d and the cross-sectional averaged velocity V are constant independently of the longitudinal position for a prismatic channel. The application of the momentum equation in the x-direction yields a relationship between the normal velocity and bed slope for a wide rectangular channel (Henderson, 1966):

$$V = \sqrt[3]{\frac{8\times g}{f}\times q\times \sin\theta}, \tag{A1}$$

where f is the Darcy–Weisbach friction and q is the discharge per unit width: q = Q/B.

In gradually varied steady flows, the backwater equation for a flat channel assuming hydrostatic pressure distribution expresses the variation with distance of the water depth d:

$$\frac{\partial d}{\partial x}\times\left(1-\frac{Q^2}{g\times B^2\times d^3}\right) = \sin\theta-\frac{f}{D_H}\times\frac{V^2}{2\times g}. \tag{A2}$$

Using the continuity equation, it becomes

$$V = \sqrt[3]{\frac{8\times q}{f}\times\left(g\times\sin\theta + V\times\frac{\partial V}{\partial x}\times\left(\frac{g\times d}{V^2}-1\right)\right)}. \tag{A3}$$

Assuming that V × ∂V/∂x is very small, Equation A3 may be rewritten in a form that holds for both uniform equilibrium flow and gradually varied flows:

$$\frac{\partial V}{\partial \theta}\approx\frac{1}{3}\times\sqrt[3]{\frac{8\times g}{f}}\times q\times(\sin\theta)^{-2/3}. \tag{A4}$$

If the fluid velocity is V_o on a horizontal slope, assuming for a small bed slope (sinθ ≈ θ), the linearization of Equation A4 gives

$$V\approx V_o+\frac{1}{3}\times\sqrt[3]{\frac{8\times g}{f}\times q\times \sin\theta}. \tag{A5}$$